Ab Initio and Semiempirical Studies on the Transition Structure of the Baeyer and Villiger Rearrangement. The Reaction of Acetone with Performic Acid†

Renán Cárdenas,* Raúl Cetina, Jaime Lagúnez-Otero, and Lino Reyes

Instituto de Química, Universidad Nacional Autónoma de México, Circuito Exterior Ciudad Universitaria, Coyoacan 04510 Mexico D.F., Apartado Postal 70-213 México

Received: February 21, 1996; In Final Form: August 30, 1996⊗

Ab initio and semiempirical calculations have been performed on the reaction mechanism of the Baeyer−Villiger reaction of acetone and performic acid. They focus, at the rate-limiting step (RLS), on the structures, energies, Mulliken charges, and what we refer to as evolution of the bond orders. The geometries of the Criegee intermediate, the methyl group migration transition state structure (TSs), and the product were found and optimized with the HF/ 4-21G, the HF/4-31G, and the HF/6-31G** basis sets of double-ζ quality in the *ab initio* methodology. AM1, PM3, and MNDO were used in the semiempirical calculations. The correlation energies were also evaluated at the MP2/6-31G**//HF/4-31G and MP2/6-31G** level of theory. A discussion dealing with the nature of the transition state structure (TSs) and its determination is presented, observing that irrespective of the method of calculation, the topology of the TSs and the general orientation of the transition vectors are invariant. From the calculations *in vacuo*, by using novel methodology, we find two reactive cycles: a central one, where the oxygen bonds break in close synchronicity with the methyl group migration, and a secondary one, where a proton is transferred. This proton seems to have protected the carbonyl oxygen from the attack of the methyl group. Scanning the movement of the proton, we can observe the effect that it produces on the atoms belonging to the reactive cycles and, interestingly, the lack of effect on those that do not belong to it. Finally, by using elliptic coordinates, we see that the atoms constituting both of the reactive cycles are found on ellipsoidal surfaces where the reactive centers are the foci.

1. Introduction

The analysis of chemical kinetics is essential for the comprehension of chemical and biochemical processes.[1−3] Experimental methods such as spectroscopic techniques play an important role in obtaining data because they give quantitative and qualitative information about the stable molecular structures. However, there is important information concerning the properties of structures far from the equilibrium that is difficult to obtain experimentally.

In particular, to understand the kinetics of a given chemical reaction, it is essential to determine the characteristics of its transition state structure (TSs).[4] As it has a remarkably short half-life (10^{-15}−10^{-25} s), it is most often studied using theoretical methods.[5,6] In 1930 Eyring and Polanyi[7] used London's theory,[8,9] and later, in 1932, a kinetic treatment of the chemical reaction problem was made by Peltzer and Wigner.[10] The latter contains an important discussion of the existence of a col or saddle point on the potential energy surface (PES) corresponding to the transition state.

Even though it exists only temporarily, the activated complex has a robust structure with an invariant topology[11] on the PES characterized by having all the force constants like any normal valence force field, with one exception. This is a value in the diagonalized representation that may be small but is always negative, as we find in several calculations.[12−17]

The activated complex may differ in geometry and energy depending on the semiempirical method or the *ab initio* basis set used, but will always have the same general topology. This concept is very useful in localizing the TSs on the PES. Indeed, if the method of calculation is not pathologic, the geometries of the structure are all in a neighborhood that we call a quadric[18] domain. In the PES, the quadric region corresponds to the open neighborhood of the TSs where the hyperfunction has all concavities in the principal directions positive except for one. The radius of the neighborhood is taken as the minimum radius where these conditions are fulfilled. The negative curvature evaluated at the TSs corresponds to a path conducing to the reactant and to the product.

We are using these concepts to study the Baeyer−Villiger reaction, by which ketones are converted into esters or lactones.[19] Being important in diverse chemical disciplines including inorganic chemistry, enzymology, and drug development, it has been extensively studied experimentally and is the subject of a great quantity of papers published to date.[20] However, despite these studies, few theoretical quantum chemical works appear in the literature. The pioneering papers include the works of Stoute *et al.*[21] and Rubio *et al.*[22,23] These initial calculations were made with an *ab initio* reduced basis set and with semiempirical CNDO/2 and MINDO/3 methods. Recently Dewar[24] has published a study using AM1. Considering the limitations of the underlying approximations, semiempirical methods have been developed to a surprising level of accuracy and reliability[25,26] and are, at present, commonly used for studying large molecular systems of chemical interest.

The Reaction. The reaction studied,

$$(H_3C)_2CO + HCO_3H \rightarrow CH_3COOCH_3 + HCO_2H$$

occurs in two stages. The first step is the formation of a tetrahedral adduct known as the Criegee intermediate (Figure 1), resulting from the attack of the peracid on the ketone.[27] In this structure the carbonyl carbon is acting with sp^3 hybridization. The second step is the migration of a methyl group from

† This is Publication No. 1463 of the Institute of Chemistry of the UNAM.
* To whom correspondence should be sent.
⊗ Abstract published in *Advance ACS Abstracts,* November 15, 1996.

S1089-5639(96)00527-0 CCC: $14.00

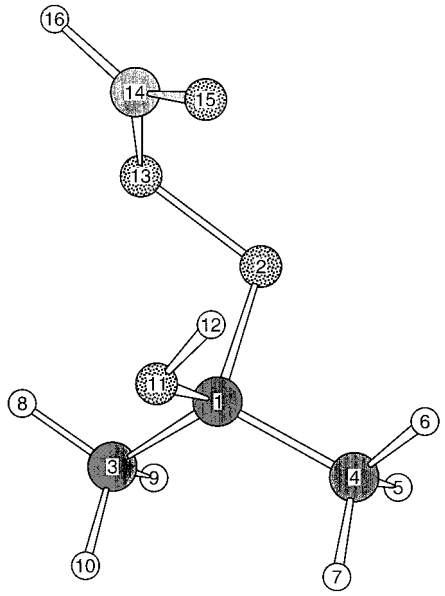

Figure 1. Criegee intermediate. It is possible to see that the C4 has a free path to reach the O2. The C4 atomic charge is smaller than the C3, H12 also has a free route to the O15. Figures have the following convention: White balls are hydrogen atoms, the black are carbon atoms, and the dotted are oxygen atoms.

the acetone moiety to one of the two peroxide oxygens of the performic acid part in the intermediate. The addition process under particular conditions has been postulated to be rate determining. However the accepted rate-limiting step (RLS) is the migration step.[28]

When the ketone is not symmetric, it is clear that there is a different migratory faculty shown by some fragments, in relation to others.[20] The methyl ketones generate acetates because the methyl group has a poor migratory capacity. In the case of acetone, the symmetry of the molecule allows for the migration of either one of the two methyl groups.

In the migration step, the process begins with the Criegee intermediate, ending with the production of ester and formic acid or, in presence of solvents, with the conjugated acid of ester and formic acid ion. Stoute *et al.*[21] have discussed the possible existence of a synchronous path between the methyl migration and the breaking process of the equivalent bond between the two oxygens of the peroxy acid carbonyl part (they used OH and OF instead of the peracid moiety). Unfortunately they did not reach any clear conclusion with respect to the putative synchronicity.

In this paper we report a theoretically characterized Criegee intermediate and the transition state structure (TSs) for the methyl migration step of the Baeyer−Villiger reaction between the performic acid and the acetone molecule. We are continuing a new line of theoretical studies with methodologies available today, trying to elucidate the reaction mechanism and possible new trends within it.

In particular we describe the process by which a methyl group attacks one oxygen of the peroxide and not the oxygen of the ketone carbonyl. The hypothesis studied by Stoute *et al.*[21] and Rubio *et al.*[22] asserts that the carbonyl oxygen is blocked by a proton. We test this hypothesis with higher levels of theory.

We consider that the geometry and mechanism of the reaction can be calculated adequately if there are no contradictions in the topology nor in the mechanism, using different *ab initio* HF and semiempirical methods. Andrés *et al.*[29] show this for the addition reaction of CO_2 with $CH_3NHCONH_2$. We should mention, however, that we are aware that to obtain deeper

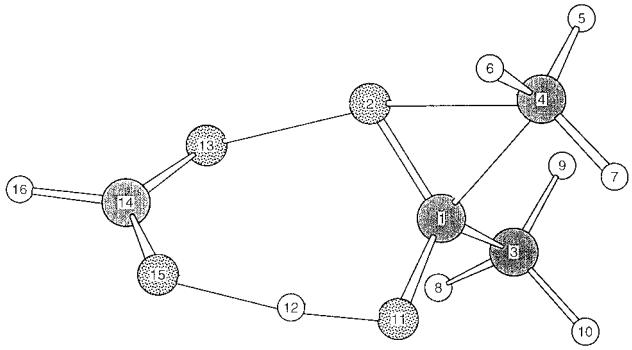

Figure 2. RLS transition state. Single black lines represent bonds that are in the breaking/creating process. The methyl group C4 is migrating to the O2. H12 is reaching the O15 to form the formic acid. The O2−O13 bond is breaking.

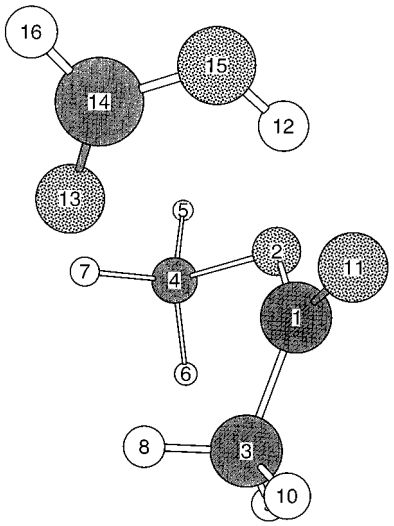

Figure 3. Product of the reaction. In the bottom part of the drawing is the ester and in the top part, the formic acid. The H12 is still pointing to the O11.

knowledge on the electronic properties and energy, it should be evaluated with CASCF or CCSD(T) methods.

Representation of chemical reactions using internal coordinates and energy leads to the understanding of the reaction path, but the term reaction coordinate is not always clear. The most accepted reaction path presently is the Fukui trajectory,[30] but we must observe that this path is essentially static. In fact, in some reactions it is clear that this trajectory is not followed by the reaction.[31,32] Furthermore a chemical understanding of the path in terms of the geometry is difficult to achieve.

The representation of the stationary points of the reaction path in terms of the evolution in the bond orders, as formulated by Mayer,[33] has been made in a modified More O'Ferrall−Jencks diagram.[29,34−36] It seems to be a fruitful representation of the characteristic points. We used this kind of analysis to elucidate characteristics of the trajectory in the reaction. In this manner it was possible to consider the existence of the synchronous path between the methyl migration and other bond breaking/making processes.

2. Methodology and Models

The quantum mechanical calculations were performed at the *ab initio* HF-SCF level. The basis set used is the double-ζ split valence type, and the correlation energy was taken into consideration with the Møller−Plesset method.

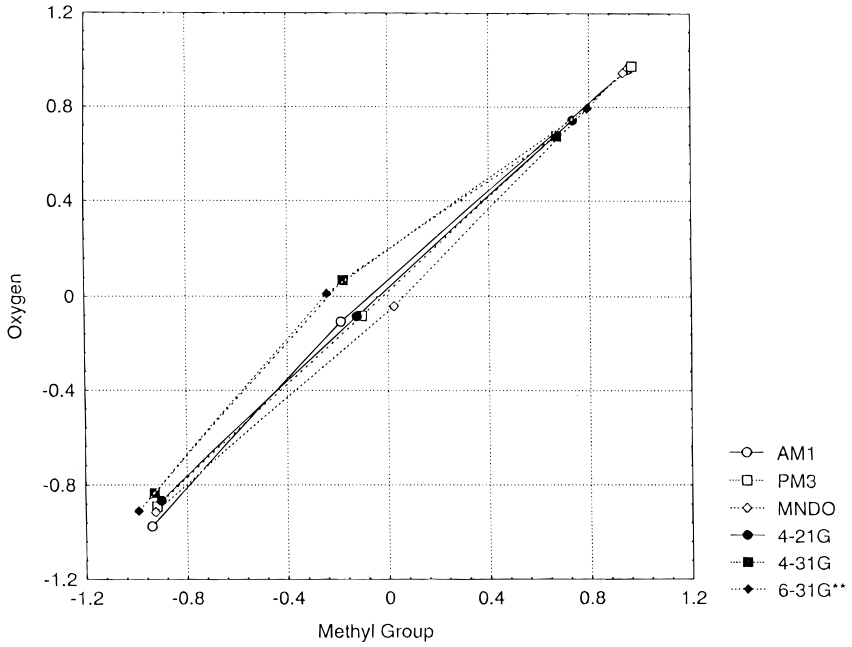

Figure 4. Bond order evolution of methyl group *vs* oxygen. Comparing the bond change of the methyl carbon, C4, and the oxygen, O2, we see that lines run close to the diagonal with slope = 1. This gives evidence of a synchronicity between the two processes.

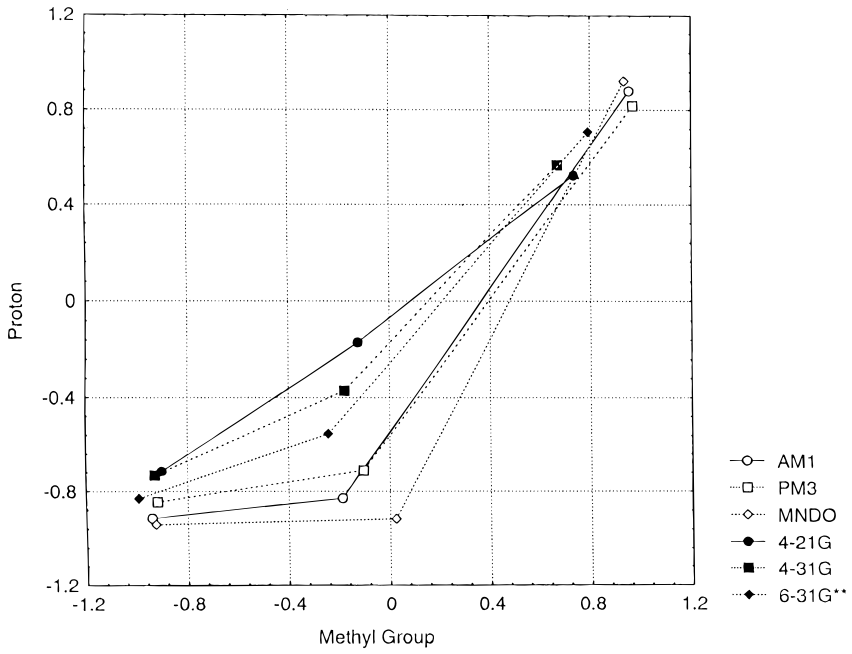

Figure 5. Bond order evolution of methyl group *vs* proton. It is possible to see by the downward inflexion of the lines that, at the TS, the bond change of the methyl group is more advanced than that of the proton H12.

The characteristic structures were calculated using the program MONSTERGAUSS[37] with basis sets 4-21G,[38] 4-31G,[39] and 6-31G**[40] and single-point calculations 6-31G**/4-31G, MP2/6-31G**//4-31G, and MP2/6-31G** with the GAUSSIAN 92 programs.[41] Three semiempirical methods have been used: MNDO,[42] AM1,[43] and PM3.[44]

In the process of achieving the Criegee intermediate a proton is expected to be donated by either an acid medium, water molecules, or any protonic element to the acetone carbonyl oxygen. Evaluating the intermediate, a saddle point can be found corresponding to a structure with sp^3 hybridization in the carbonyl carbon. However, as we discuss below, this theoretical tetrahedral complex cannot resist the methyl group migration. Indeed, we could not find the completely optimized protonated Criegee structure as a minimum. Therefore we have considered a neutral Criegee intermediate, where the proton that protects the carbonyl oxygen has been transferred from the peracid (Figure 1).

The minimum energy structures have been calculated with the standard minimization procedures Conjugated Gradients[45] and the Berny method.[46] The TSs has been calculated by diagonalizing the force constant matrix; in the last step of the procedure we consider 42 variables using the subroutine VA05[47] with analytic gradients. We have used the program package MOPAC6[48] to work the semiempirical methods, optimization procedures to minimize have been the standard one, FLEPO, and in the search of the TS we used the SIGMA program and the FORCE subroutine to characterize the point.

Optimization has been made with the first three basis sets, following the procedures until the gradient lengths became

TABLE 1: Criegee Intermediate Geometry

	4-21G	4-31G	6-31G**	AM1	PM3
total energy (au)	−454.433 970	−454.818 099	−455.506 102	−69.903 303	−65.059 491
		Distances			
O2−C1	1.4861	1.4699	1.4276	1.4600	1.4122
C3−C1	1.5153	1.5061	1.5165	1.5118	1.5338
C4−C1	1.5264	1.5166	1.5220	1.5210	1.5437
O11−C1	1.4124	1.3990	1.3781	1.4036	1.4059
H12−O11	0.9661	0.9553	0.9466	0.9693	0.9493
O13−O2	1.4648	1.4221	1.3838	1.2905	1.5607
C14−O13	1.3712	1.3538	1.3323	1.3880	1.3415
O15−C14	1.1955	1.1954	1.1771	1.2241	1.2068
		Bond Angles (deg)			
C3−C1−O2	110.8	110.8	111.3	112.1	115.3
C4−C1−O2	101.4	101.7	102.3	104.7	103.9
O11−C1−O2	109.3	109.0	110.0	104.1	106.0
H12−O11−C1	111.0	113.7	109.7	107.9	108.5
O13−O2−C1	108.9	110.4	110.6	113.0	109.9
C14−O13−O2	111.0	112.9	112.4	115.4	112.0
O15−C14−O13	126.5	126.5	127.2	119.3	123.0
		Dihedral Angles (deg)			
C4−C1−O2−C3	122.2	122.4	121.3	123.2	121.4
O11−C1−O2−C4	119.1	119.1	119.5	119.8	119.4
H12−O11−C1−O2	−46.5	−52.5	−51.5	−60.9	−61.0
O13−O2−C1−H11	−57.6	−57.7	−58.3	−57.5	−67.3
C14−O13−O2−C1	97.8	99.8	101.9	97.3	119.4
O15−C14−O13−O2	−8.7	−7.7	−4.9	−6.1	−3.8

TABLE 2: Geometry of the Methyl Group Migration[a] Transition State

	4-21G	4-31G	6-31G**	AM1	PM3
total energy (au)	−454.342 333	−454.731 291	−455.418 281	−69.817 456	−65.010 187
		Distances (Å)			
O2−C1	1.3466	1.3155	1.2886	1.3131	1.3202
C3−C1	1.5035	1.4904	1.5039	1.4929	1.5035
C4−C1	1.8444	1.8452	1.7673	1.9242	1.9619
O11−C1	1.3186	1.3252	1.3155	1.3563	1.3322
H12−O11	1.0936	1.0158	0.9864	0.9857	0.9808
O13−O2	1.9043	1.9445	1.8979	1.8559	1.7682
C14−O13	1.2694	1.2730	1.2579	1.2991	1.2887
O15−C14	1.2620	1.2490	1.2231	1.2535	1.2396
		Bond Angles (deg)			
C3−C1−O2	117.0	118.9	118.8	124.8	125.0
C4−C1−O2	74.1	75.7	76.8	73.3	66.6
O11−C1−O2	117.8	117.8	118.1	115.4	114.5
H12−O11−C1	111.0	113.0	108.6	110.2	110.6
O13−O2−C1	104.7	104.7	106.9	113.3	116.0
C14−O13−O2	109.9	109.6	109.4	107.1	112.9
O15−C14−O13	126.3	125.8	127.5	120.1	120.5
		Dihedral Angles (deg)			
C4−C1−O2−C3	104.5	105.6	106.1	102.7	98.2
O11−C1−O2−C4	106.5	104.8	106.4	102.5	105.3
H12−O11−C1−O2	21.9	19.9	16.6	2.0	10.0
O13−O2−C1−H11	−69.4	−70.6	−71.4	−77.1	−73.5
C14−O13−O2−C1	82.0	85.2	85.3	96.3	84.1
O15−C14−O13−O2	−29.5	−29.5	−24.0	−16.1	−19.0

[a] Other relevant parameters of the geometry 6-31G**: See text. Distances (Å): C1−C14 = 3.15, O2−C4 = 1.935, C14−C4 = 4.370, C14−O2 = 2.602, C1−O15 = 3.072, O11−O15 = 2.578, H12−O15 = 1.627. Dihedral angles (deg): O2−C1−C14−O13 = 58.0, O11−C1−C14−O15 = 23.7, C4−C1−C14−O13 = 93.4.

smaller than 1×10^{-4} mdyn. The reaction paths were explored with the Conjugated Gradients subroutine. Beginning from the TSs we followed down the reaction path until the reactant and product were reached.

The methodology to explore the potential energy surface (PES) can be described as a combination of searching for minima and characterizing the curvature of stationary points by calculating the Hessian at these points and diagonalizing the force constant matrix. The directions following the eigenvector corresponding to the negative eigenvalue were explored. In this way, it was possible to find the reactant and the product of the reaction step.

The charge was evaluated by the Mulliken procedure, and the bond orders were evaluated following the Mayer formulation.[33] Calculations were made with Silicon Graphics 4-35D and CRAY YMP/432 computers.

The proton force scan was made with the 6-31G** basis set.

Modified More O'Ferrall−Jencks Diagrams. The problem of determining the degree of advance of the reaction in terms of the electronic density can be studied by using the atomic charge and the bond orders. In this reaction three atomic movements are considered: (a) the methyl migration, (b) the breaking of the bond between two oxygens, and (c) the transfer of a proton from the lactone moiety to the formic acid part.

TABLE 3: Charge Distribution in the Reactants, TS, and Product

	4-21G	4-31G	6-31G**	AM1	PM3	MNDO
Reactant Atom Charge						
C1	0.54	0.49	0.57	0.17	0.22	0.21
O2	−0.33	−0.34	−0.35	−0.16	−0.12	−0.19
Me3	0.10	0.14	0.08	0.08	0.03	0.08
Me4 Tr.	0.09	0.11	0.06	0.06	0.05	0.06
O11	−0.73	−0.74	−0.64	−0.34	−0.38	−0.33
H12	0.43	0.43	0.36	0.23	0.24	0.20
O13	−0.44	−0.43	−0.33	−0.14	−0.17	−0.17
C14	0.72	0.64	0.63	0.25	0.38	0.35
O15	−0.61	−0.55	−0.52	−0.32	−0.37	−0.32
H16	0.23	0.22	0.15	0.18	0.11	0.11
Charge Transfer						
formic acid moiety	−0.10	−0.12	−0.07	−0.03	−0.05	−0.03
Transition State Atom Charge						
C1	0.71	0.59	0.63	0.24	0.36	0.23
O2	−0.25	−0.23	−0.25	−0.08	−0.08	−0.07
Me3	0.13	0.19	0.14	0.14	0.10	0.15
Me4 Tr	0.23	0.29	0.25	0.25	0.12	0.18
O11	−0.79	−0.76	−0.64	−0.31	−0.32	−0.26
H12	0.52	0.52	0.45	0.30	0.30	0.24
O13	−0.68	−0.68	−0.63	−0.41	−0.44	−0.43
C14	0.71	0.64	0.63	0.27	0.42	0.36
O15	−0.76	−0.75	−0.69	−0.51	−0.54	−0.46
H16	0.19	0.17	0.09	0.11	0.07	0.05
Charge transfer						
formic acid moiety	−0.54	−0.62	−0.60	−0.54	−0.49	−0.48
Product Atom Charge						
C1	0.97	0.89	0.82	0.30	0.38	0.34
O2	−0.72	−0.74	−0.60	−0.27	−0.23	−0.32
Me3	0.06	0.09	0.02	0.09	0.08	0.09
Me4 Tr.	0.42	0.45	0.38	0.20	0.17	0.22
O11	−0.70	−0.66	−0.61	−0.32	−0.37	−0.33
H12	0.49	0.51	0.41	0.27	0.26	0.23
O13	−0.68	−0.62	−0.57	−0.38	−0.42	−0.38
C14	0.72	0.64	0.60	0.26	0.38	0.36
O15	−0.77	−0.75	−0.59	−0.32	−0.35	−0.31
H16	0.20	0.20	0.12	0.17	0.10	0.10
Charge Transfer						
*formic acid moiety**	−0.04	−0.02	−0.03	0.00	−0.03	0.00

A methodology that has been reported recently[29] is used. It consists in observing the changes in bond orders among the stationary points: reactive, transition state, and product. We have obtained two diagrams (Figures 4, 5) contrasting the three atomic movements:

Atomic movement	*xy* correlation (bonds forming minus breaking)	graph
a *vs* b	$x = n(\text{C4O2}) - n(\text{C1C4})$, $y = n(\text{C4O2}) - n(\text{O2O13})$	Figure 4
a *vs* c	$x = n(\text{C4O2}) - n(\text{C1C4})$, $y = n(\text{O15H12}) - n(\text{O11H12})$	Figure 5

These graphs compare the evolution of some relevant bonds in the reaction by plotting the values of the differences between their orders (in this case, in the Mayer formulation). An analysis of the slopes of these diagrams has been made in order to quantify the degree of synchronicity of the movements.

3. Discussion and Conclusions

The Criegee Intermediate. Table 1 shows the geometry of this adduct and Table 3 the charge distribution calculated with the basis sets and methods above. It is a tetrahedral complex formed by the addition of the acetone molecule and the performic acid (Figure 1). From the point of view of the PES, this intermediate is the reactant for the RLS of the reaction.

Some distances not included in Table 1 show an important characteristic. The distance from O11 to O13 is 2.699 Å, from O11 to O15 2.963 Å, from H12 to O11 0.946 Å, from H12 to O13 2.896 Å, and from H12 to O15 2.441 Å. It can be seen from this intermediate that the H12 is ready to form the bridge with O15 in the TS, but it is not yet formed.

TABLE 4: Transition Vectors

	basis set eigenvalue	6-31G** −2.51	4-31G −1.95	4-21G −2.71	av −2.39
(ρ)	**O2−C1**	**−0.189**	**−0.165**	**−0.174**	**−0.176**
	C3−C1	−0.007	−0.008	−0.001	−0.005
	C4−C1	**0.278**	**0.34**	**0.283**	**0.300**
	H5−C4	−0.006	−0.004	−0.003	−0.004
	H6−C4	−0.005	−0.003	−0.002	−0.003
	H7−C4	−0.01	−0.009	−0.009	−0.009
	H8−C3	−0.004	−0.002	−0.003	−0.003
	H9−C3	0.000	0.001	0.002	0.001
	H10−C3	0.000	0.000	0.000	0.000
	O11−C1	**−0.101**	**−0.113**	**−0.149**	**−0.121**
	H12−O11	**0.123**	**0.193**	**0.413**	**0.243**
	O13−O2	**0.573**	**0.533**	**0.492**	**0.533**
	C14−O13	**−0.101**	**−0.101**	**−0.132**	**−0.111**
	O15−C14	**0.092**	**0.099**	**0.135**	**0.109**
	H16−C14	0.008	0.003	−0.001	0.003
(θ)	C3−C2−O1	0.072	0.059	0.032	0.054
	C4−C1−O2	**−0.556**	**−0.539**	**−0.507**	**−0.534**
	H5−C4−C1	0.027	0.032	0.03	0.030
	H6−C4−C1	0.029	0.024	0.046	0.033
	H7−C4−C1	**−0.221**	**−0.219**	**−0.183**	**−0.208**
	H8−C3−C1	−0.056	−0.051	−0.042	−0.050
	H9−C3−C1	0.01	0.015	0.015	0.013
	H10−C3−C1	0.015	0.015	0.011	0.014
	O11−C1−O2	0.028	0.02	0.001	0.016
	H12−O11−C1	−0.036	−0.039	−0.026	−0.034
	O13−O2−C1	**−0.185**	**−0.218**	**−0.19**	**−0.198**
	C14−O13−O2	**−0.109**	**−0.098**	**−0.097**	**−0.101**
	O15−C14−O13	−0.062	−0.06	−0.076	−0.066
	H16−C14−O15	−0.079	−0.074	−0.088	−0.080
(**τ**)	C4−**C1−O2−C3**	**−0.184**	**−0.186**	**−0.164**	**−0.178**
	H5−C4−C1−C3	0.008	0.01	0.001	0.006
	H6−C4−C1−O2	0.036	0.028	0.028	0.031
	H7−C4−C1−H5	0.009	0.012	0.003	0.008
	H8−C3−C1−O2	0.001	0.001	0.002	0.001
	H9−C3−C1−H8	−0.015	−0.016	−0.011	−0.014
	H10−C3−C1−H8	0.005	0.007	0.005	0.006
	O11−C1−O2−C4	**−0.164**	**−0.162**	**−0.123**	**−0.150**
	H12−O11−C1−O2	0.047	0.051	0.043	0.047

We have seen above that the intermediate can be theoretically built by protonation of the carbonyl oxygen of the acetone, followed by the formation of the tetrahedral complex. The symmetric saddle point structure shows a very weak bond between the acetone and the peracid, which would be the first one to break if the methyl group were forced to migrate. Therefore, it can be expected that the protonation of the carbonyl oxygen occurs at the same time as the peracid loses a proton. Experiments[49] with ^{18}O in the carbonyl group show that this oxygen is found in the ester or the lactone at the end of the reaction. One hypothesis explaining this is that this oxygen is protected by the proton attached to it.

The calculated structure of the neutral Criegee intermediate (Figure 1) shows that of the oxygens in the complex only the one in the hydroxyl of the peracid (the strand oxygen O2) is available. This has a main role in the reaction.

Of the two methyl moieties, one of them (C4) shows a clear and shorter path to reach this oxygen. The other methyl group is blocked by the peracid part (Figure 1). It is interesting to note that these methyl groups will have an inversion in the Mulliken charge as the reaction occurs. They will pass from 0.06 for the C4 group and 0.08 for the C3 group in the Criegee intermediate to 0.25 and 0.14, respectively, in the TS, with the 6-31G** basis set. The semiempirical methods show the same tendency with the exception of PM3. Another interesting

TABLE 5: Energies and Energy Barriers in the RLS

basis set	Criegee intermediate	TS methyl group migration	product
4-21G	−454.433 970 h	−454.342 333 h	−454.520 676 h
	0.0 kcal/mol	57.5 kcal/mol	−54.4 kcal/mol
			−111.9*[a]
4-31G	−454.818 099	−454.731 291	−454.918 641
	0.0 kcal/mol	54.5	−63.1
			−117.6*
6-31G**	−455.506 102	−455.418 490	−455.618 679
	0.0	54.9	−70.6
			−125.6*
6-31G**/4-31G	−455.500 20	−455.413 865	−455.613 877
	0.0	54.2	−71.3
			−125.5*
MP2/6-31G**/4-31G	−456.788 111	−456.732 599	−456.882 856
	0.0	34.8	−59.4
			−94.3*
MP2/6-31G**	−456.781 001	−456.733 117	−456.881 246
	0.0	30.0	−62.9
			−92.9*
AM1	−69.903 303	−69.817 456	−70.015 584
	0.0	53.9	−70.4
			−124.3*
PM3	−65.059 491	−65.010 187	−65.163 972
	0.0	31.0	−65.6
			−96.5*
MNDO	−70.254 945	−70.111 315	−70.360 664
	0.0	90.1	−66.3
			−156.5*

[a] $*E = E(\mathrm{TS}) - E(\mathrm{PR})$. h = Hartrees.

TABLE 6: TS Force Scan Variation for the Movement of H12 (6-31G)[a]**

		distance					
	parameter	−0.2	0.2	0.4	0.8	1.2	1.6
(ρ)	O2−C1	−0.04	0.14	0.35	−0.43	−7.02	−6.59
	C3−C1	0.00	−0.01	−0.02	−0.04	−0.06	−0.06
	C4−C1	0.01	−0.02	−0.05	−0.08	−0.09	−0.10
	O11−C1	−0.09	0.16	0.41	0.66	−3.72	−14.74
	H12−O11	−2.93	0.37	0.01	0.64	5.63	−2.32
	O13−O2	0.03	0.04	0.12	−0.90	−8.55	−9.40
	C14−O13	−0.08	0.17	0.36	0.15	1.51	14.26
	O15−C14	0.11	−0.24	−0.58	−0.33	8.07	19.14
	H16−C14	0.00	0.01	0.03	0.06	0.08	0.05
(Θ)	C3−C1−O2	0.00	0.02	0.04	0.07	0.08	0.09
	C4−C1−O2	−0.01	0.09	0.19	0.32	0.36	0.38
	O11−C1−O2	−0.05	0.27	0.72	−0.84	−19.98	−34.54
	H12−O11−C1	−0.07	0.14	0.37	0.10	−14.16	−40.06
	O13−O2−C1	−0.06	0.23	0.58	0.87	−13.11	−12.32
	C14−O13−O2	−0.06	0.26	0.64	−1.38	−17.32	−16.58
	O15−C14−O13	−0.04	0.15	0.34	−0.86	−6.75	2.75
	H16−C14−O15	−0.02	0.03	0.07	0.12	0.13	0.08
(τ)	C4−C1−O2−C3	−0.01	0.02	0.04	0.07	0.08	0.09
	O11−C1−O2−C4	−0.01	0.01	0.03	0.06	0.07	0.08
	H12−O11−C1−O2	0.03	−0.08	−0.22	0.22	10.75	29.77
	O13−O2−C1−O11	0.05	−0.19	−0.53	0.58	19.96	47.09
	C14−O13−O2−C1	−0.05	0.20	0.49	−0.85	−8.57	0.99
	O15−C14−O13−O2	−0.01	0.04	0.10	0.09	−0.52	3.24
	H16−C14−O15−O13	0.00	−0.01	−0.01	−0.02	−0.01	0.00

[a] Distances are in Å. Values are gradients in -mdyn.

observation is that all these methods mantain the same charge sign. The formic acid moiety is almost neutral.

The Quadric Region. The potential energy surface (PES) is defined as a multivariable real function, where the domain of the function contain $3N-6$ or $3N-5$ real coordinates. These coordinates can be expressed internally or in a Cartesian way with restrictions such as the Eckart conditions.[11c,50]

The surface around the saddle point is a hyperbolic paraboloid with $3N-6$ coordinates in the domain. It is possible to find an open neighborhood where the same characteristics of the Hessian are fulfilled; this region is the quadric surface bounded by an inflection region. If we calculate the square of the derivatives of the PES function in the canonical directions, we can transform the problem of searching for a minimax into a problem of minimization. In the last years, the more common molecular quantum mechanics methods used to calculate the PES have shown good behavior, and the molecular geometries differ by less than 10%.[51] This gives us the possibility of evaluating one geometry obtained from any method and transferring it to another in order to search for the TSs.

Transition Vectors. To evaluate the differences in directions of the three *ab initio* derived transition vectors (TV),[53] we built

TABLE 7: Evolution in Bond Orders for Methyl Migration, Oxygen Break, and Hydrogen Transfer

	Me Δ of C4O2−C1C4			O Δ of C4O2−O2013			H Δ of H12O15−H12O11		
	R	TS	P	R	TS	P	R	TS	P
4-21G	−0.902	−0.125	0.734	−0.865	−0.085	0.743	−0.715	−0.170	0.524
4-31G	−0.930	−0.179	0.669	−0.834	0.068	0.675	−0.732	−0.371	0.568
6-31G**	−0.993	−0.243	0.792	−0.909	0.011	0.792	−0.831	−0.553	0.708
AM1	−0.941	−0.188	0.955	−0.974	−0.107	0.961	−0.914	−0.829	0.879
PM3	−0.920	−0.104	0.969	−0.890	−0.082	0.974	−0.845	−0.711	0.817
MNDO	−0.926	0.023	0.935	−0.914	0.041	0.946	−0.940	−0.916	0.922
av	−0.935	−0.136	0.842	−0.898	−0.026	0.848	−0.829	−0.592	0.736

TABLE 8: Slopes and Differences in Angles of the Lines TS-R and P-TS

	O/ME TS-R *m*(TS-R)	O/Me P-TS *m*(P-TS)	Δθ	H/Me TS-R *m*(TS-R)	H/Me P-TS *m*(P-TS)	Δθ
4-21G	1.003	0.964	1.1	0.701	0.808	−3.9
4-31G	1.201	0.716	14.6	0.481	1.107	−22.2
6-31G**	1.227	0.754	13.8	0.371	1.218	−30.0
AM1	1.151	0.934	6.0	0.113	1.494	−49.7
PM3	0.990	0.984	0.2	0.164	1.424	−45.6
MNDO	1.006	0.992	0.4	0.025	2.015	−62.2
av	1.09	0.89	5.1	0.31	1.34	−35.6

an average, normalized TV (see last column of Table 4). The angles between the different vectors and this average are less than 8°, corresponding to a projection of 0.982. The smallest projection between the vectors is 0.973. This invariance of the vectors indicates an independence from the basis set used.

Notably, the small basis set 4-21G overplays the role of the proton H12, as is possible to see also in the More O' Ferrall diagram (Figure 5).

We have observed a subspace containing the principal weight of the vector (see values in boldface in Table 4). It is composed of 14 variables, the majority of which form the reactive cycles. The principal variations belonging to the methyl C4 coordinates, 0.620, and to the bond O13−O2, 0.602. A similar trend is followed by the three basis sets; the relation between this movement is 1.03, showing simultaneity between the two movements. In contrast, the proton H12 makes a small contribution to the TV (0.123). These values can be observed with the basis set 6-31G**, in agreement with the More O' Ferrall diagram (Figure 4).

Energy Profile. Table 5 shows the energies calculated with three different basis sets 4-21G, 4-31G, and 6-31G** and three single-point calculations: HF/6-31G**//4-31G, MP2/6-31G**//4-31G, and MP2/6-31G**. It can be observed that the energies with the 6-31G** and 6-31G**//4-31G are comparable. This means that the TS is not so sensitive to the geometry. The same can be seen with MP2/6-31G** and MP2/6-31G**//4-31G, where the difference is less than 5 kcal.

The difference in correlation energy between the TS and the reactant is approximately 25 kcal/mol smaller than the difference found with the HF procedure. The comparison between the HF/6-31G** //4-31G energies shows a barrier of 54.2 kcal from the reactant and 125 kcal/mol from the product; the optimized energy with 4-21G is 57.5, with 4-31G is 54.5, and with 6-31G** is 54.9 kcal/mol. The large correction to the energy arises when the correlation perturbation term MP2 is taken into account.

The energy barrier values have a significant dispersion among the calculations. Therefore we conclude that a higher level of calculation such as CSSD(T) or CASCF should be performed; however, we can affirm that the reaction is exothermic. This is derived from observing the differences between the energies of the initial reactant (acetone + performic acid) and of the product (ester + formic acid). Using basis sets 4-21G, 4-31G, and 6-31G**, at the HF level, they are 76.2, 79.2, and 95.1 kcal/mol respectively. Considering perturbation theory, MP2/6-31G** gives a diference of 110.5 kcal/mol in this sense.

The Product. Following the reaction path, it is possible to arrive at the structure identified as the product of the reaction (Figure 3); the ester and formic acid. Our theoretical results are in agreement with the experiments[49] using isotope ^{18}O in the carbonyl acetone that show that the oxygen is found in the ester carbonyl or the lactone carbonyl at the end of the reaction.

Elliptic Coordinates. To study regions of electronic and nuclear configurational space, elliptic coordinates can be used. They can help describe the movement of a given component of the system that is exchanged between a donor and acceptor (see, for example, ref 54 and more recently ref 55). We used these coordinates to represent the reactive cycles in the TSs where the foci of the main cycle are C1 and O2; C4 would be the element interacting between these two centers. We find that the sum of the distances C1−C4 + C4−O2 tends to be constant. It is 3.7 Å in the Criegee intermediate, 3.9 Å in the TSs, and 3.8 Å in the product, giving an average of 3.8 Å, with a differences of less than 3%.

In the final product, it is possible to see a general symmetry. As they both have a central carbon with two oxygens, one with a single bond and another with a double bond, the two central structures in the formic acid and the ester seem to have played similar roles in the reaction. The carbon C1 in the ester and the carbon C14 in the formic acid work as donor and acceptor in the electronic flux. In the TSs, we can consider them as the foci of an ellipsoid. Expressing the coordinates of the atoms that form the secondary cycle in terms of the distances to these carbons, we can see that there are two groups of atoms whose sum of distances to these carbons have small variations. The sums of the distances O2−C1 + O2−C14 and O13−C1 + O13−C14 are 3.89 and 3.84 Å, respectively, with a difference of less than 0.6%. The addition of the distances O11−C1 + O11−C14, H12−C1 + H12−C14, and O15−C1 + O15−C14 gives an average of 4.32 Å and a difference of less than 3%. This implies that the atoms in both circuits do lie on ellipsoidal surfaces.

It is interesting to note that in the TSs the proton bridging O11 and O15 is found close to the ellipse generated by the two main centers of the reaction (C1 and C14), in a compromise with the expected trajectory between its acceptor and donor foci

(O11 and O15). This points to the importance of the other atoms in the reaction.

Force Scan by Proton Transfer. To test the effects of the proton transition from the acetone moiety to the formic acid on the neighboring atoms and observe the role played by carbons C1 and C14 as transmitters of electronic flux, a scan (Table 6) was made of variable 11 (*r*H12−O11). This was performed over the distance traversed by the proton, freezing the atoms and calculating their forces as a function of the displacement.

As a first observation, it can be seen that, in general, the forces increase significantly when the proton comes closer to the formic acid. The first two columns of Table 6 represent a small vicinity around the TSs. It is notable that the force at −0.2 Å, the H12−O11 bond, is relatively large, a consequence of the anharmonicity; however, the effect on the other forces behaves as expected.

The variations in the forces on the methyl protons are small and almost constant and have therefore been omited from Table 6. The movement of the H12 in the direction of the product generates forces on the other atoms that would push the complete structure to the product if it were allowed to relax: the methyl C4 tends to increase its bond length and to close its angle as the O11 forms a double bond and tends to reduce its bond distance.

The O13 appears to have an erratic behavior, but an inspection of Table 6 shows that in the vicinity of the TSs the protonation of O15 causes the C14−O15 bond to become single and simultaneously slightly increase the bond strength of O13−O2. Only when the reaction is more advanced is it possible to see a clear tendency for this bond to break. Indeed, this is another way to understand the graphs of Figures 4 and 5, where the lack of synchronicity between the proton and both the methyl and the O13 is shown.

A similar analysis can be made with the other members of the reactive cycle: O11, O2, O15, C1, and C14, showing behaviors without contradictions. It is clear to see that the atoms involved in the reactive cycles are affected by the scan. In contrast, H16 and C3 do not show sensitivity to the movement of the proton. This also provides evidence for their absence from the reactive cycles.

Modified More O'Ferrall−Jencks Diagrams and the Evolution of the Bond Orders. We present two diagrams considering the methyl migration, the O−O bond breaking, and the proton transfer (Figures 4 and 5). A straight line between the reactive state, the TS, and the product means that there is a precise syncronicity. On the other hand, if the reaction is not symmetric, with the angles between the broken lines differing significantly, we must consider the existence of a lack of synchronization.

In the comparison of the methyl migration *vs* the O−O bond break, the data distribution shows a slight dispersion around the straight line. The semiempirical methods show differences in the average angle of less than 3° and in the *ab initio* calculations of less than 10°. In contrast, it is clear by the defined angles in Figure 5 that the proton transfer occurs after those events have taken place.

Using the basis set 4-21G, the proton transfer shows an anomalous behavior; it could originate from the small size of the basis set as well.

We can also express the degree of advance of the reaction by observing the average differences in bond orders, found in row 7 of Table 7. Theoretically, if the average at the TS is close to zero, we can infer that the atom binds the donor and the receptor with approximately the same order. If the average is negative, it implies that it is associated more with the donor than the receptor. Correspondingly, if it is positive, then the opposite is true. Like the graphs, the row shows that while the proton H12 is still tightly associated with its donor, O11, at the TS, the methyl group has already advanced toward the O2.

References and Notes

(1) Glasstone S.; Laidler, K.; Eyring H. M *The Theory of Rate Processes;* McGraw-Hill: New York, 1941.

(2) Laidler, K. *Theories of Chemical Reaction Rates;* McGraw-Hill: New York, 1969.

(3) Truhlar, D. G.; Hase, W. L.; Hynes, J. T. *J. Phys. Chem.* **1983**, *87*, 2664.

(4) Williams, I. *Chem. Soc. Rev.* **1993,** 277.

(5) Skancke, A. *Acta. Chem. Scand.* **1993,** *47*, 629.

(6) Andrés, J.; Moliner, V.; Domingo, L. R.; Picher, M. T.; Krechl, J. *J. Am. Chem. Soc.* **1995,** *117*, 8807.

(7) Eyring, H.; Polany, M. *Z. Phys. Chem., Abt. B* **1932**, *12*, 279.

(8) Heitler, W.; London, F. *Z. Physik.* **1927**, *44*, 55.

(9) London, F. *Z. Electrochem.* **1929**, *35*, 552.

(10) Pelzer, H.; Wigner, E. *Z. Phys. Chem., Abt. B* **1932**, *15*, 445.

(11) We have used the term topology in reference to connectivity. Geometry would not be an acceptable term because small changes in, for example, a dihedral angle can produce displacements in atoms far from the rotation axis. In such cases the differences in geometry can be more than 1 Å, but connectivity or topology is maintained. In general it is difficult to speak about invariant geometry. The following references can help in determining the correct the usage of the term topology: (a) Peterson, M. R.; Csizmadia, I. G. In *Molecular Stucture and Conformation Progress in Theoretical Organic Chemistry;* Csizmadia, I. G., Ed.; Elsevier Scientific Publishing Co.: Amsterdam, 1982; Vol. III, Chapter V. (b) Francis, G. K. *A Topological Picturebook*; Springer-Verlag: New York, 1987; pp 1−9. (c) Mezey, P. G. *Potential Energy Hypersurfaces;* Elsevier: Amsterdam, 1987; Section 1.2, pp 6−18.

(12) Andrés, J.; Cardenas, R.; Silla, E.; Tapia, O. *J. Am. Chem. Soc.* **1988**, *110*, 666.

(13) Tapia, O.; Lluch, J. M.; Cardenas, R.; Andrés, J. *J. Am. Chem. Soc.* **1989**, *111*, 829.

(14) Tapia, O.; Cardenas, R.; Andrés, J.; Colonna-Cesari F. *J. Am. Chem. Soc.* **1988**, *110*, 4046.

(15) Tapia, O.; Cardenas, R.; Andrés, J.; Krechl, J.; Campillo M.; Colonna-Cesari F. *Int. J. Quantum Chem.* **1991,** *39*, 6, 767.

(16) Jacob, O.; Cardenas, R.; Tapia, O. *J. Am. Chem. Soc.* **1990**, *112*, 8692.

(17) Tapia, O.; Andrés, J.; Cardenas, R. *Chem. Phys. Lett*. **1992**, *189*, 4, 5, 395.

(18) As we are speaking about surfaces (a PES), a better term than quadratic is quadric. The term quadratic is more acceptable for mathematical forms than for geometric ones. The following references elucidate this difference: (a) Thomas, G. B., Jr. *Calculus and Analytic Geometry*, 4th ed.; Addison-Wesley Publishing Co.: Menlo Park, CA, 1969; Section 12: 11, pp 413−417. (b) Shilov, G. E. *An Introduction to the Theory of Linear Spaces*; Prentice-Hall, Inc.: Englewood Cliffs, NJ, 1961; Chapters 10, 11, pp 195−243. (c) Boehm, W.; Prautzsch H. *Geometric Concepts for Geometric Design*; A K Peters: Wellesley, MA, 1994; Chapters 13 and 18. (In this book exists a clear definition of the two concepts.) (d) Korn, G. A.; Korn, T. M. *Mathematical Handbook for Scientists and Engineers*; McGraw-Hill Book Co.: New York, 1961; pp 71−79, pp 368−373.

(19) Baeyer, A.; Villiger, V. *Ber. Dtsch. Chem. Ges.* **1899**, *32*, 3625.

(20) Krow, G. R. In *Organic Reactions*; Paquette *et al*., Eds.; John Wiley & Sons, Inc.: New York, 1993; Vol. 43, p 254.

(21) Stoute,V. A.; Winnik, M. A.; Csizmadia, I. G. *J. Am. Chem. Soc.* **1974**, *96*, 6388.

(22) Rubio, M.; Cetina, R.; Bejarano,A. *Afinidad* **1983,** *40*, 176.

(23) Rubio, M.; Reyes, L.; Cetina, R.; Pozas, R. *Afinidad* **1989,** *46*, 341.

(24) Dewar, M. J. S.; Hwang, J. C.; Kuhn. D. R *J. Am. Chem. Soc.* **1991,** *113*, 735.

(25) Stewart, J. J. P. In *Reviews in Computational Chemistry*; Lipkowitz, K. B., Boyd, D. B., Eds.; VCH Publishers: New York, 1990; Vol. 1, pp 45−82.

(26) Zerner, M. C. In *Reviews in Computational Chemistry*; Lipkowitz, K. B., Boyd, D. B., Eds.; VCH Publishers: New York, 1991, Vol. 2, pp 313−366.

(27) Criegee, R. *Justus Liebigs Ann. Chem.* **1948**, *560*, 127.

(28) Hawthorn, M. F.; Emmons, W. D. *J. Am. Chem. Soc*. **1958,** *80*, 6398, and references cited therein.

(29) Andrés, J.; Moliner, V.; Krechl, J.; Silla, E. *J. Phys. Chem.* **1994**, *98*, 3664.

(30) Fukui, K. *J. Phys. Chem.* **1970**, *74*, 4161.

(31) Miller, W. H.; Handy, N. C.; Adams, J. E. *J. Chem. Phys.* **1980**, *72*, 99.

(32) Miller, W. H. In *New Theoretical Concepts for Understanding Organic Reactions;* NATO ASI Series; Academic Pub.: Dordrecht, 1989; pp 347−372.
(33) Mayer, I. *Int. J. Quantum Chem*. **1986**, *29*, 477.
(34) Varandas, A. J. C.; Formosinho, S. J. *J. Chem. Soc*., *Faraday Trans. 2* **1986,** *82*, 953−962.
(35) Lendvay, G. *J. Mol. Struct.* (*THEOCHEM*) **1988,** *167*, 331.
(36) Lendvay, G. *J. Phys. Chem.* **1989**, *93*, 4422.
(37) Peterson, M. R.; Poirier R. A. *MONSTERGAUSS*; University of Toronto: Ontario, Canada, 1988.
(38) Pulay, P.; Fogarasi, G.; Pang, F.; Boggs, J. E. *J. Am. Chem. Soc*. **1979**, *101*, 2550.
(39) Ditechfield, R.; Hehre, W. J.; Pople J. A. *J. Chem. Phys*. **1971**, *54*, 724.
(40) Hehre W. J.; Ditechfield, R.; . Pople, J. A. *J. Chem. Phys*. **1972**, *56*, 2257.
(41) Frisch, A. M. J.; Trucks, G. W.; Head-Gordon, M.; Gill, P. M. W.; Wong, M. W.; Foresman, J. B.; Johnson, B. G.; Schlegel, H. B.; Robb, M. A.; Replogle, E. S.; Gomperts, R.; Andrés, J. L.; Raghavachari, K.; Binkley, J. S.; Gonzalez, C.; Martin, R. L.; Fox, D. J.; Defrees, D. J.; Baker, J.; Stewart, J. J. P.; Pople, J. A. *GAUSSIAN 92*, Revision; Gaussian, Inc.: Pittsburgh, PA, 1992.
(42) Dewar, M. J. S.; Thiel, W. *J. Am. Chem. Soc.* **1977**, *99*, 4899, 4907.
(43) Dewar, M. J. S.; Zoebisch, E. G.; Healy. E. P.; Stewart, J. J. P. *J. Am. Chem. Soc*. **1985**, *107*, 3902.
(44) Stewart, J. J. P. *J. Comput. Chem*. **1989**, *10*, 209.
(45) Davidon, W. C. *Math. Programing* **1975**, 9.
(46) Schlegel, H. B. *J. Comput. Chem*. **1982**, *3*, 214.
(47) Powell, M. J. D. *VA05 Program*, Harweel Suroutine Library. Atomic Energy Research Establishment: Harweel, U.K.
(48) Stewart, J. J. P. *MOPAC6 Manual*, 6th ed.; USA AF Academy: CO 80840, 1990.
(49) Token, K.; Hirano, K.; Yokoyama, T.; Goto K. *Bull. Chem. Soc. Jpn.* **1991**, *64*, 2771.
(50) Eckart, C. *Phys. Rev*. **1935,** *47*, 552.
(51) Levy, M.; Perdew, J. *J. Chem. Phys.* **1986**, *84*, 4519.
(52) Stahl, K. W.; Köster, F. E. *Experientia* **1984**, *40*, 734.
(53) McIver, J. W., Jr. *Acc. Chem. Transition Vectors* **1974,** *7*, 72.
(54) Burrau, O. *Det. Kgl. Danske Vid. Selskab*. **1927,** *7*, 1.
(55) Tapia, O.; Andrés, J. L. *J. Mol. Struct. (THEOCHEM)* **1995,** *335*, 267.

JP960527R